Cume 355 is based on the paper *"Metallicity Gradients and Gas Flows in Galaxy Pairs"*, by Lisa Kewley etal., 2010, ApJ 721, L48. Exam prepared by R. Walterbos.

~~Please answer the following questions, carefully explaining each answer.~~

Total number of points: 65
Expected passing grade: 45

1a. (5 pts) In the introduction they mention that large, interaction-induced gas flows would dilute the central metallicity of luminous galaxies. Why is this so?

1b. The authors write in the introduction "We find that between the first and second pericenter (i.e. ~ 1Gyr), the metallicity gradient becomes significantly flattened and that the central metallicity becomes diluted by infalling low-metallicity gas." I think what they meant to say is "between the first and second pericenter passage".

(i) (5 pts) What do they mean with "peri-center passage"?

(ii) (10 pts) Show that for the galaxies in their sample, one might indeed expect of order 1Gyr to pass between peri-center passages. Please make sure to state any assumptions or estimates you make in addressing this question.

2. In the section on observations, the authors discuss the number of lines per mm for the red and blue grating or grism, and then state the spectral resolution for the two sides.

a. (5 pts) What is a "dichroic"? Why would it be used?

b. (10 pts, evenly distributed over questions (i) through (iv)) The number of lines per mm is the parameter that controls the dispersion of the spectroscopic setup; think of this as over how wide an angle the light is dispersed as a function of wavelength. This, with the rest of the spectrograph optics and the details of the CCD detector determines how many Angstroms per pixel we get. In imaging, we would talk about the plate scale: how many arcsec per pixel. More dispersion implies fewer Angstroms per pixel. A related, but different, parameter is the resolution of the spectrograph, which determines how well we can resolve spectral lines (the equivalent quantity in imaging is the Point Spread Function, or PSF). The resolution is affected by the dispersion but also by other parameters, most notably for a given spectrographic setup, by the slit width used.

(i) Draw a sketch of a spectrum with some emission lines in it and indicate what is meant with the resolution and how we would measure it from the spectrum to determine it.

(ii) Why do we generally use a slit with a spectrograph? What would a slit-less spectrum of an observation of a region of the sky with stars and galaxies in it look like?

(iii) If I increase the number of lines per mm on a grating, does the spectrograph's dispersion go up or down (if we observe in the same spectroscopic order)? You might draw a sketch to help explain your answer. How would that generally affect the resolution?

(iv) How does the resolution of a spectrum change with the width of the slit (i.e. does it generally get better or worse when I observe with a wider slit)? Explain.

c. (5 pts) Why do the observed spectra need to be corrected for extinction? What type of extinction(s) can you think of and how do they affect the spectra?

3. In section 3, the authors discuss the distances of the HII regions. They refer here to the distance of an HII region to the center of the galaxy it belongs to. They write "Our distances take inclination into account using the optical diameters, inclinations, and line-of-nodes position angles from ~~Hyperleda ...." For line of nodes here, you can simply think of "the major axis of a galaxy on the~~ sky".

a. (5 pts) Sketch the geometry, indicating inclination, and line of nodes. Let's say that an HII region has coordinates (ρ,ϑ) on the sky, where the center of the galaxy is at (0,0), ρ is the angular distance from the galaxy center to the HII region, and ϑ is the angle between the line of nodes (which runs through the galaxy center of course) and the line between HII region and galaxy center.

b. (5 pts) ~~Calculate the~~ Find the expression for radial distance r, which is the distance of the HII region to the galaxy center in the plane of the galaxy, for the HII region at (ρ,ϑ) in a galaxy with an inclination i. You should find (still in terms of an angular distance since I am not asking you to factor in the galaxy's distance to us):

$$r = \rho\left(\cos^2\theta + \frac{\sin^2\theta}{\cos^2 i}\right)^{\frac{1}{2}}$$

c. (5 pts) For which angle theta is the uncertainty in the derived r the largest? For what range of inclination is the uncertainty highest, for inclinations between 5 to 15, or between 70 to 85. Comment.

4. Let's look at the results.

a. (5 pts) Why do they define the results in terms of the slope as defined in Table 1, footnote d. In particular, why do they divide the metallicity slope by (delta R/R_25)? Couldn't they have just used delta_R instead? What do they do with that parameter in the analysis?

b. (5 pts) Why are the inclinations relevant to the topic of this paper? Comment on this as a potential source of uncertainty on the results, considering for example what you see in the grey-scale panels in Figure 1.

The Astrophysical Journal Letters, 721:L48–L52, 2010 September 20 doi:10.1088/2041-8205/721/1/L48

METALLICITY GRADIENTS AND GAS FLOWS IN GALAXY PAIRS

Lisa J. Kewley[1], David Rupke[1], H. Jabran Zahid[1], Margaret J. Geller[2], and Elizabeth J. Barton[3]
[1] Institute for Astronomy, 2680 Woodlawn Drive, University of Hawaii, Hilo, HI 96822, USA; kewley@ifa.hawaii.edu
[2] Smithsonian Astrophysical Observatory, 60 Garden Street, Cambridge, MA 02138, USA
[3] University of California, Irvine, CA 92697, USA
Received 2010 June 19; accepted 2010 August 11; published 2010 August 30

ABSTRACT

We present the first systematic investigation into the metallicity gradients in galaxy close pairs. We determine the metallicity gradients for eight galaxies in close pairs using H ii region metallicities obtained with high signal-to-noise multi-slit observations with the Keck LRIS Spectrograph. We show that the metallicity gradients in close pairs are significantly shallower than gradients in isolated spiral galaxies such as the Milky Way, M83, and M101. These observations provide the first solid evidence that metallicity gradients in interacting galaxies are systematically different from metallicity gradients in isolated spiral galaxies. Our results suggest that there is a strong relationship between metallicity gradients and the gas dynamics in galaxy interactions and mergers.

Key words: galaxies: abundances – galaxies: fundamental parameters – galaxies: interactions – galaxies: starburst

1. INTRODUCTION

Galaxy interactions and mergers are fundamental to the formation and evolution of galaxies. Current *N*-body/smoothed particle hydrodynamic (SPH) simulations predict that, as a merger progresses, galaxy disks become disrupted by tidal effects, causing large gas inflows into the central regions where kiloparsec-scale starbursts may be triggered (Barnes & Hernquist 1996) or active galactic nuclei (AGNs) may be fueled (Springel et al. 2005; Hopkins et al. 2006). At very late stages, starburst- or AGN-driven superwinds may drive gas back out of the central regions (Narayanan et al. 2008).

Evidence for major gas inflows in interacting galaxies has been seen in ionized gas (Rampazzo et al. 2005), in neutral gas (Hibbard & van Gorkom 1996; Georgakakis et al. 2000; Iono et al. 2005; Emonts et al. 2006; Cullen et al. 2007), and in kinematic studies using absorption lines (Rupke et al. 2005; Martin 2006). Whether large-scale gas flows occur may depend on the mass difference between the interacting galaxies (see, e.g., Woods et al. 2006; Horellou & Koribalski 2007). In Kewley et al. (2006a), we compared the nuclear gas-phase metallicities of nearby field galaxies with nearby galaxy pairs. We found that close pairs have systematically lower metallicities than either field galaxies or more widely separated pairs at the same luminosity (see also Lee et al. 2004). Most isolated late-type spiral galaxies and starburst barred spirals display strong metallicity gradients (see Henry & Worthey 1999 for a review). We proposed a merger scenario in which galaxy interactions drive large gas flows toward the central regions, carrying less enriched gas from the outskirts of the galaxy into the central regions, disrupting metallicity gradients, and diluting central metallicities.

Subsequent research into central metallicities of interacting galaxies confirms the relationship between galaxy interactions and central metallicities. Rupke et al. (2008) show that merging luminous infrared galaxies have lower central metallicities compared with local isolated galaxies of similar luminosity or mass, suggesting that large interaction-induced gas flows have diluted the central metallicity of luminous infrared galaxies. Similarly, Ellison et al. (2008) and Michel-Dansac et al. (2008) showed that galaxy pairs in the Sloan Digital Sky Survey have lower central metallicities for their stellar mass than isolated galaxies. Outliers from the standard mass–metallicity relation for star-forming galaxies have been shown to be morphologically disturbed (Peeples et al. 2009; Sol Alonso et al. 2010). Additional investigations suggest a relationship between large-scale environment and metallicity (Cooper et al. 2008; Ellison et al. 2009).

Chien et al. (2007) investigated the stellar population ages and metallicities of 12 young star clusters in the merging galaxy pair NGC 4676. They found a relatively flat distribution of oxygen abundances along the northern tail, suggesting efficient gas mixing within the tail. Trancho et al. (2007) and Bastian et al. (2009) find similarly flat metallicity distributions in star clusters in the merging galaxies NGC 3256 and the Antennae, respectively.

Theoretical simulations that include the effect of mergers on the metallicity distribution in galaxies support the picture of major gas inflows induced by the tidal effects of galaxy interactions. In Rupke et al. (2010a), we used *N*-body/SPH simulations to investigate the theoretical relationship between metallicity gradients and galaxy major mergers. These simulations are based on close passage, equal-mass disk galaxy merger models with a range of initial geometries and initial pericenters. We find that between first and second pericenter (i.e., $\sim$1 Gyr), the metallicity gradient becomes significantly flattened and that the central metallicity becomes diluted by infalling low-metallicity gas.

Recently, Montuori et al. (2010) used major merger simulations to show that the circumnuclear metallicities become diluted after the first pericenter passage due to major gas inflows. These model predictions are consistent with observations by Kewley et al. (2006a), Rupke et al. (2008), and with the simulations of Rupke et al. (2010a). Montuori et al. find a second gas dilution peak at final coalescence in major mergers and significant central metallicity dilution in galaxy fly-bys, highlighting the importance of the gas-phase metallicity for tracing the recent merger or interaction history of galaxies.

To date, metallicity gradients have been investigated for relatively small numbers of star clusters and H ii regions in a small number of interacting galaxies. In this Letter, we present the first systematic investigation of metallicity gradients in interacting galaxies. We present Keck LRIS spectra for H ii regions in eight galaxies in close pairs selected on the basis of their position on the luminosity–metallicity relation. We show

Table 1
Sample Galaxies

ID	Common Name	Coordinates (J2000)	M_B	Nuclear Class[a]	Hubble Type[b]	Separation (kpc)[c]	Central log(O/H)+12[a]	R_{25} (kpc)	Gradient Slope (R/R_{25})[d]
1	UGC 12914	00 01 38.3 +23 29 01	−20.88	H II	S(r)cd? pec	17.4	9.08	14.69	-0.104 ± 0.048
2	UGC 12915	00 01 41.9 +23 29 45	−20.09	...	S?	17.4	...	11.11	...
3	UGC 312	00 31 23.9 +08 28 01	−20.53	H II	SB?	21.1	8.78	11.67	-0.133 ± 0.079
4	UGC 813	01 16 16.4 +46 44 25	−20.44	H II	Sb	16.5	9.00	11.16	-0.233 ± 0.045
5	UGC 816	01 16 20.5 +46 44 53	−20.78	H II	S?	16.5	8.91	13.33	-0.252 ± 0.032
6	NGC 3994	11 57 36.9 +32 16 39	−19.85	C	SA(r)c pec	24.7	8.93	6.18	-0.139 ± 0.045
7	NGC 3995	11 57 44.1 +32 17 39	−20.67	H II	SAm pec	24.7	8.75	19.40	-0.339 ± 0.059
8	UGC 12545	23 21 41.9 +27 04 15	−20.01	H II	SBcd	21.9	8.88	11.81	-0.381 ± 0.157
9	UGC 12546	23 21 41.2 +27 05 14	−20.03	AMB	Sbc	21.9	8.91	10.64	-0.421 ± 0.094

Notes.
[a] Spectral classes and central metallicities are derived from nuclear long-slit spectral fluxes from Barton et al. (2000). We use the Kewley et al. (2006b) spectral classification scheme and the Kewley & Dopita (2002) [N II]/[O II] metallicity calibration.
[b] Hubble Types are obtained from the NASA Extragalactic Database.
[c] Separation refers to the projected separation of the pair or projected distance to the closest galaxy in the n-tuple.
[d] Gradient slope is defined in terms of $\frac{\Delta \log(\mathrm{O/H})}{\Delta R/R_{25}}$, where R_{25} is the B-band isophote at a surface brightness of 25 mag arcsec^{-2}.

that all close pair galaxies have significantly flatter metallicity gradients than metallicity gradients measured in isolated spiral galaxies. We suggest that flat metallicity gradients provide a "smoking gun" for recent major gas flows in interacting galaxies. Throughout this Letter, we adopt the flat Λ-dominated cosmology as measured by the *Wilkinson Microwave Anisotropy Probe* experiment ($h = 0.72$, $\Omega_m = 0.29$; Spergel et al. 2003).

2. SAMPLE SELECTION AND OBSERVATIONS

We selected five luminous ($M_B < -20$) sets of close pairs (separation between 15 and 25 kpc) from the Barton et al. (2000) galaxy pairs sample. Our pairs were selected to (1) span a range of positions on the luminosity–metallicity relation in Kewley et al. (2006a), (2) contain at least one galaxy with suitable orientation for metallicity gradient analysis, and (3) to span a range of galaxy properties that may influence metallicity gradients (pair separation, presence of bars, and Hubble type). In Table 1, we list our sample galaxies and their properties.

We obtained spectra for 12–40 star-forming regions in eight of our close pair galaxies with the Keck Low-Resolution Imaging Spectrograph (LRIS). Slit masks were designed using 1″ wide slits based on Hα images of the target galaxies observed with the Vatican Advanced Technology Telescope (E. Barton & R. Jansen 2010, private communication). We used the 560 nm dichroic with the 900 l mm^{-1} red grating and the 600 l mm^{-1} grism, giving a spectral resolution of 3.5 Å FWHM between 3500 and 5500 Å and 2.8 Å between 5500 and 7000 Å.

The spectra were reduced using a custom pipeline developed in IRAF and IDL that includes standard bias subtraction, flat fielding, rectification, and wavelength calibration. Spectra were flux calibrated using standard stars observed at a similar airmass and time to the slit mask observations. We derived emission-line fluxes from each spectrum using UHSPECFIT, a spectral line-fitting routine developed by us. For continuum fitting, UHSPECFIT utilizes code from Moustakas (2006) and the González Delgado et al. (2005) evolutionary stellar population synthesis models.

Emission-line fluxes were corrected for extinction using the Cardelli et al. (1989) extinction curve. The majority of our H II region spectra do not have the electron temperature-sensitive auroral [O III] λ4363 line, which is only produced in high electron temperature, low-metallicity regions. We derived metallicities [in units of log(O/H)+12] using the strong emission lines. For the N II λ6584 O II λ3727 ratios covered by our sample [log([N II]/[O II]) > -1.3; log(O/H) + 12 > 8.4], the [N II]/[O II] ratio is a strong function of metallicity with very little ($\ll$0.1 dex) dependence on the ionization state of the gas. We use the Kewley & Dopita (2002) [N II]/[O II] calibration to derive metallicities for the H II regions in our sample, after removal of spectra potentially contaminated by an AGN or other non-thermal sources according to the Kewley et al. (2006b) classification scheme. More details on the spectroscopic pipeline, UHSPECFIT, emission-line flux measurements and classification are provided in Rupke et al. (2010b).

Kewley & Ellison (2008) show that large discrepancies exist among metallicities derived using different strong-line calibrations. These discrepancies are systematic, therefore relative metallicities such as gradients may be reliably compared if the same calibration is used. In addition, we have verified that we obtain the same results if independent metallicity calibrations based on different line ratios are applied such as the [O III]/Hβ [N II]/Hα calibration by Pettini & Pagel (2004), and the R_{23} calibrations by Kobulnicky & Kewley (2004) and McGaugh (1991).

3. ANALYSIS

In Figure 1, we show the position of our sample pairs on the luminosity–metallicity relation (where possible) and the spatial distribution of metallicities for each galaxy (colored circles). Galaxy ID numbers are given in Table 1. Spatial distributions of metallicities range from flat (e.g., NGC 3994, no. 6) to relatively steep toward the central regions (e.g., UGC 12546, no. 9).

We measure metallicity gradients for the eight pair galaxies with at least 10 H II region metallicity measurements. Galactocentric radii are computed using the direct distance to the galaxy center, where the galaxy center is defined using Two Micron All Sky Survey (2MASS) images from a well-defined bulge. Our distances take inclination into account using the optical diameters, inclinations, and line-of-nodes position angles from HyperLeda (Paturel et al. 2003), with double-checks on the position angles by visual inspection of H I maps, where available. Figure 2 shows the metallicity gradients (in R/R_{25}) for the close pair galaxies in our sample. The H II region radius is given

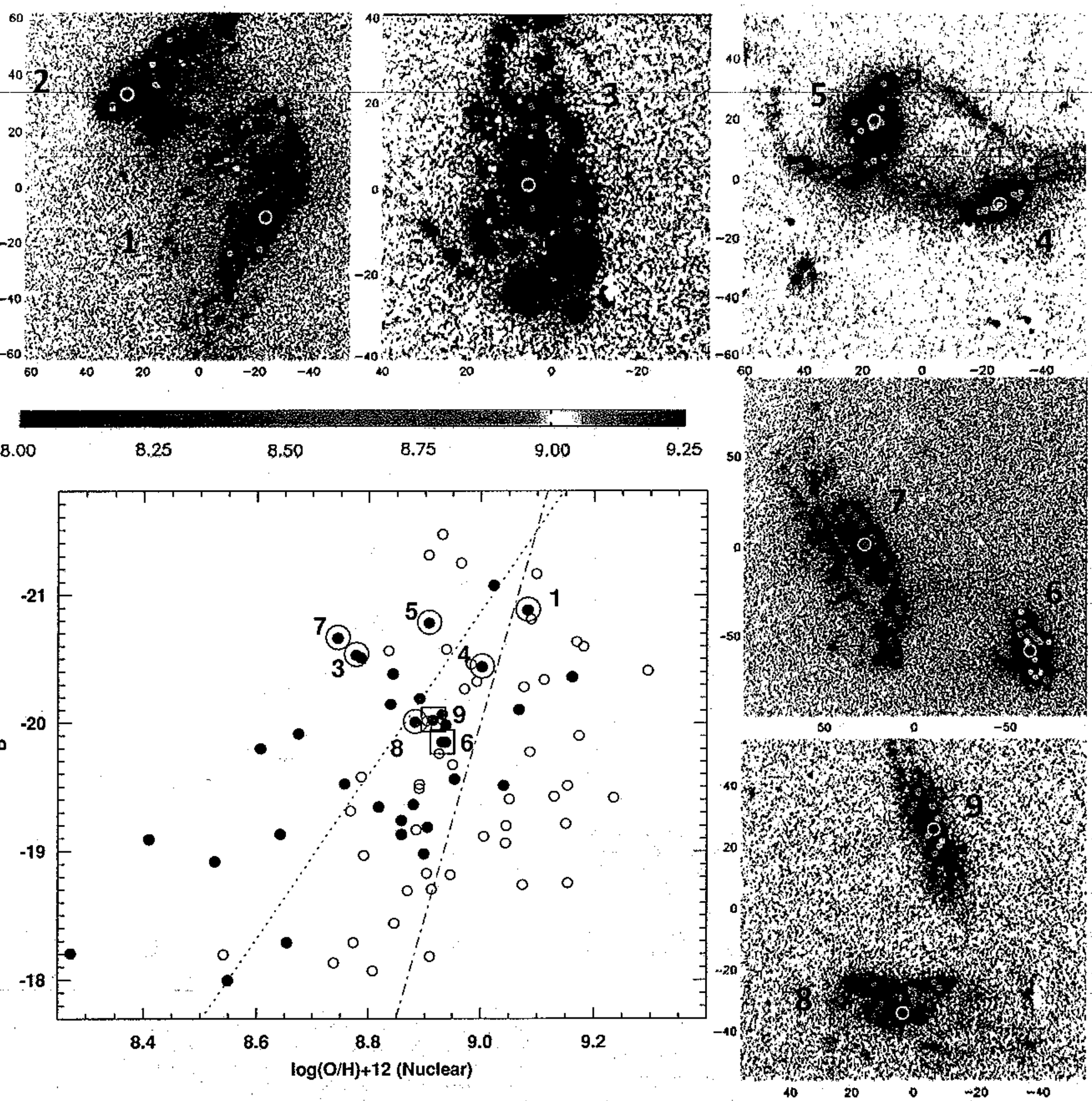

Figure 1. *B*-band luminosity-metallicity (*L–Z*) relation from Kewley et al. (2006a) for the close pair members (red) compared with isolated field galaxies from the Nearby Field Galaxy Survey (unfilled circles). All metallicities in the *L–Z* relation are calculated from spectroscopy with a central long-slit aperture that covers approximately 10% of the galaxy *B*-band light (~1 kpc). The eight close pairs with metallicity gradients (Table 1) are indicated on the *L–Z* relation as star-forming galaxies (circle outlines) and composite or ambiguous galaxies (square outlines). Top and right panels indicate the location and metallicity of the star-forming regions in each galaxy on Hα images. Metallicity colors are shown in the legend bar in units of log(O/H) + 12 and the coordinates for each panel are given in units of arcseconds. Unfilled white circles indicate the galaxy center determined using 2MASS images.

in units of R/R_{25}, where R_{25} is the *B*-band isophote at a surface brightness of 25 mag arcsec^{-2}.

We directly compare the metallicity gradients measured for our close pairs in Figure 3 for both the Kewley & Dopita (2002) [N II]/[O II] and McGaugh (1991) R_{23} calibrations. For comparison, solid lines indicate the metallicity gradients measured in the isolated spiral galaxies M101, M83, and the Milky Way. For consistency, we recalculate the H II region metallicities in the isolated spiral galaxies using the Kewley & Dopita (2002) [N II]/[O II], and McGaugh (1991) calibrations using the H II region emission-line fluxes from Shaver et al. (1983; Milky Way), Kennicutt et al. (2003; M101), and Bresolin et al. (2005, 2009; M83). The metallicity gradients in these comparison galaxies are representative of isolated spiral galaxies (see review by Henry & Worthey 1999). We note that we obtain the same results relative to the comparison galaxies if distance between the H II location and the galaxy center is defined in kiloparsecs.

The metallicity gradients of all of our close pairs are flatter than the gradients observed in the three isolated spiral comparison galaxies, regardless of calibration used. The mean gradient in our close pairs is $\frac{\Delta \log(\mathrm{O/H})}{\Delta R/R_{25}} = -0.25 \pm 0.02$ compared with

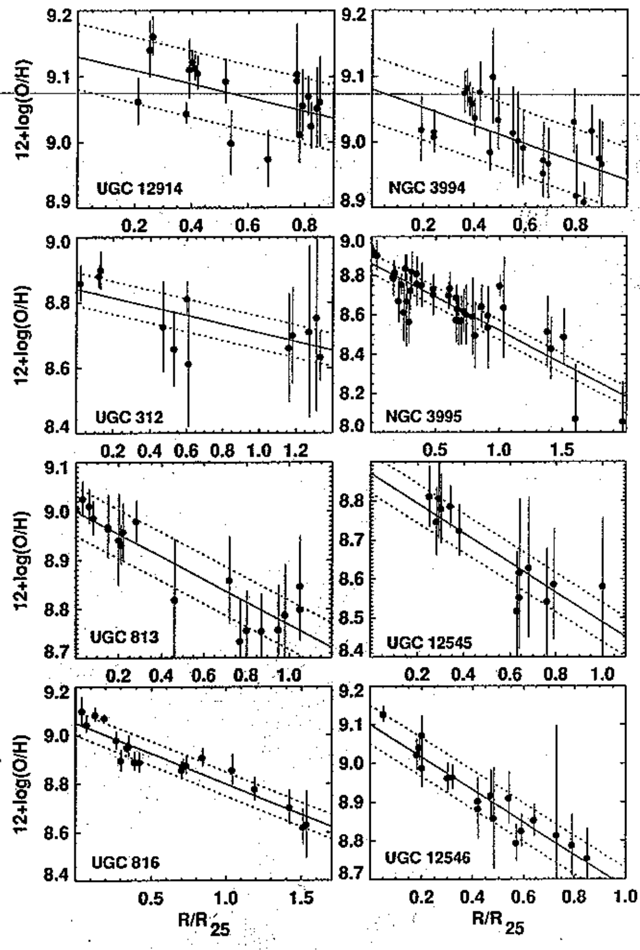

Figure 2. Metallicity gradients derived for our close pair galaxies. Solid lines indicate the least-squares line of best fit to the metallicity gradient and the dotted lines represent the average rms error (0.05 dex) about the line of best fit. The metallicity gradients are given in terms R/R_{25}, where R is the radius and R_{25} is the radius of the B-band isophote at a surface brightness of 25 mag arcsec^{-2}. Similar gradients are obtained using radius in kiloparsecs. The same gradients are obtained within the errors if alternative metallicity calibrations are applied (see Rupke et al. 2010b for a detailed comparison).

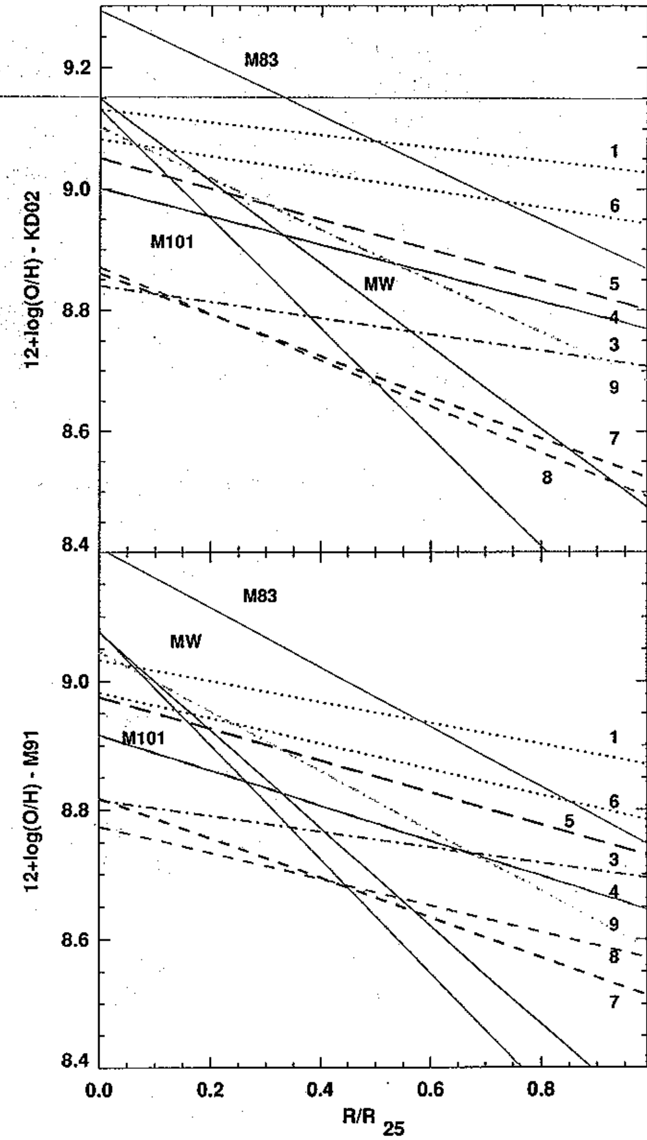

Figure 3. Metallicity gradients for the eight close pair galaxies in our sample that have metallicities measured for >10 H II regions. Galaxies are labeled according to Table 1. All metallicity gradients are least-squares fits to H II region metallicities measured using the Kewley & Dopita (2002) [N II]/[O II] calibration (top panel) and the McGaugh (1991) R_{23} calibration (bottom panel). For comparison, we show the metallicity gradients for three isolated spiral galaxies: Milky Way (black), M83 (red), and M101 (blue). The eight close pairs have substantially flatter metallicity gradients than the isolated spiral galaxies, providing a smoking gun for major merger-induced gas flows.

a mean gradient of $\frac{\Delta \log(O/H)}{\Delta R/R_{25}} = -0.67 \pm 0.09$ for the isolated spiral galaxies. In Rupke et al. (2010b), we show that the mean metallicity gradient for a large sample of 11 isolated spiral galaxies is $\frac{\Delta \log(O/H)}{\Delta R/R_{25}} = -0.57 \pm 0.05$. These results provide the first direct evidence that the metallicity gradients in galaxy pairs are systematically different from gradients in isolated spiral galaxies. Recent infall of less enriched gas from the outskirts of the close pair galaxies is the likely culprit.

In Rupke et al. (2010a), we investigate the effect of gas inflows on metallicity gradients in theoretical merger simulations. We assume the simplest conditions: no ongoing star formation, equal-mass progenitors, and small gas mass fractions. In these theoretical models, we find a dramatic flattening of the initial radial metallicity gradient between first and second pericenter. This flattening reflects the effects of gas redistribution over the galaxy disks, including both metal-poor inflow and the growth of tidal tails that carry metals out to large radius.

If large merger-triggered gas flows drive the bulk of the inflowing gas into the central kiloparsec, triggering a burst of star formation, a recent nuclear burst of star formation may be associated with a flatter metallicity gradient. Barton Gillespie et al. (2003) applied stellar population synthesis models to the $B - R$ colors and Balmer equivalent widths of the galaxy pairs sample to derive the fraction of R-band light originating from a recent burst of star formation, termed the central burst strength. In Kewley et al. (2006a), we showed that central burst strength correlates strongly with central metallicity in close pairs. This result is consistent with the theoretical simulations of Montuori et al. (2010), which show that pairs experiencing the strongest bursts of star formation also have the strongest circumnuclear dilution. If most of the infalling gas is deposited in the central regions, we might expect a correlation between the metallicity gradient slope and central burst strength in our galaxy pairs.

However, we find no statistically significant correlation between the metallicity gradient and the central burst strength (Spearman rank coefficient of −0.14 with a two-sided probability of obtaining this value by chance of 74%). Similarly, we find no statistically significant correlation between the metallicity gradient slope and the presence of blue bulges or pair projected separation. We note that our gradient sample is limited by the small sample size, and that a larger sample is required for more robust conclusions on the relationship between the metallicity gradient slope and galaxy properties. If the lack of correlation between central burst strength and metallicity gradient slope holds for a larger sample, these results would suggest that (1) the timescale for a central starburst differs from the timescale over which the metallicity gradient remains disrupted, and/or (2) the metallicity gradient slope is strongly influenced by radial gas redistribution along the spiral arms and/or metal outflows, rather than a simple inflow into the central kiloparsec.

The presence of bars is correlated with efficient gas flows toward the nucleus in late-type spiral galaxies (e.g., Sakamoto et al. 1999; Sheth et al. 2005) and bars may be created in the early stages of a merger (Barnes & Hernquist 1991). Two galaxies in our sample have bars (UGC 312 and UGC 12545). While UGC 312 has a low central metallicity and relatively flat gradient slope ($\frac{\Delta \log(\mathrm{O/H})}{\Delta R/R_{25}} = -0.133$), UGC 12545 has a steeper gradient slope ($\frac{\Delta \log(\mathrm{O/H})}{\Delta R/R_{25}} = -0.381$) that is within the full range of gradient slopes observed in our pairs sample. It is not clear from these two galaxies whether bars allow more efficient transport of gas toward the central regions during galaxy mergers.

We find no correlation between the distance from the nearby field galaxy *L–Z* relation and the close pair metallicity gradient slope. Galaxy pairs that lie close to the field galaxy *L–Z* relation in Figure 1 may have had high central metallicities ($\log(\mathrm{O/H})+12 > 9.1$ in the Kewley & Dopita 2002 [N II]/[O II] scale) prior to the interaction. In Rupke et al. (2010a), we investigated the theoretical relationship between the metallicity gradient and central metallicities. We showed that metallicity gradients become disrupted by the interaction, followed by a dilution in the central metallicity. The observational results presented here support this scenario.

4. CONCLUSIONS

We present the first systematic study of metallicity gradients in close galaxy pairs. We find that all of our galaxy pairs have flatter metallicity gradients than gradients observed in typical isolated spiral galaxies. These results show that the low central metallicities seen previously in galaxy pairs and interacting galaxies signal a relatively flat metallicity gradient. We conclude that large gas inflows are responsible for the disruption and flattening of metallicity gradients in close pair galaxies. Evidence for gas flows has been difficult to study in the past, requiring integral field or neutral gas velocity maps. Our results indicate that metallicity gradients provide a unique and feasible method for detecting recent strong tidal gas flows in galaxy interactions and mergers. Our future work includes comparisons between metallicity gradients and theoretical merger simulations and an extension of our pairs sample to later stage mergers.

We thank the referee for comments that improved this Letter. We thank Rolf Jansen for providing Hα data used for slit masks, and Li Hsin Chien for preliminary work on some of this data. The authors thank the indigenous Hawaiian community for use of their sacred mountain. This research has made use of NASA's Astrophysics Data System Bibliographic Services and the NASA/IPAC Extragalactic Database (NED).

REFERENCES

Barnes, J. E., & Hernquist, L. 1996, ApJ, 471, 115
Barnes, J. E., & Hernquist, L. E. 1991, ApJ, 370, L65
Barton, E. J., Geller, M. J., & Kenyon, S. J. 2000, ApJ, 530, 660
Barton Gillespie, E., Geller, M. J., & Kenyon, S. J. 2003, ApJ, 582, 668
Bastian, N., Trancho, G., Konstantopoulos, I. S., & Miller, B. W. 2009, ApJ, 701, 607
Bresolin, F., Ryan-Weber, E., Kennicutt, R. C., & Goddard, Q. 2009, ApJ, 695, 580
Bresolin, F., Schaerer, D., González Delgado, R. M., & Stasińska, G. 2005, A&A, 441, 981
Cardelli, J. A., Clayton, G. C., & Mathis, J. S. 1989, ApJ, 345, 245
Chien, L., Barnes, J. E., Kewley, L. J., & Chambers, K. C. 2007, ApJ, 660, L105
Cooper, M. C., Tremonti, C. A., Newman, J. A., & Zabludoff, A. I. 2008, MNRAS, 390, 245
Cullen, H., Alexander, P., Green, D. A., & Sheth, K. 2007, MNRAS, 376, 98
Ellison, S. L., Patton, D. R., Simard, L., & McConnachie, A. W. 2008, AJ, 135, 1877
Ellison, S. L., Simard, L., Cowan, N. B., Baldry, I. K., Patton, D. R., & McConnachie, A. W. 2009, MNRAS, 396, 1257
Emonts, B. H. C., Morganti, R., Tadhunter, C. N., Holt, J., Oosterloo, T. A., van der Hulst, J. M., & Wills, K. A. 2006, A&A, 454, 125
Georgakakis, A., Forbes, D. A., & Norris, R. P. 2000, MNRAS, 318, 124
González Delgado, R. M., Cerviño, M., Martins, L. P., Leitherer, C., & Hauschildt, P. H. 2005, MNRAS, 357, 945
Henry, R. B. C., & Worthey, G. 1999, PASP, 111, 919
Hibbard, J. E., & van Gorkom, J. H. 1996, AJ, 111, 655
Hopkins, P. F., Hernquist, L., Cox, T. J., Di Matteo, T., Robertson, B., & Springel, V. 2006, ApJS, 163, 1
Horellou, C., & Koribalski, B. 2007, A&A, 464, 155
Iono, D., Yun, M. S., & Ho, P. T. P. 2005, ApJS, 158, 1
Kennicutt, R. C., Bresolin, F., & Garnett, D. R. 2003, ApJ, 591, 801
Kewley, L. J., & Dopita, M. A. 2002, ApJS, 142, 35
Kewley, L. J., & Ellison, S. L. 2008, ApJ, 681, 1183
Kewley, L. J., Geller, M. J., & Barton, E. J. 2006a, AJ, 131, 2004
Kewley, L. J., Groves, B., Kauffmann, G., & Heckman, T. 2006b, MNRAS, 372, 961
Kobulnicky, H. A., & Kewley, L. J. 2004, ApJ, 617, 240
Lee, J. C., Salzer, J. J., & Melbourne, J. 2004, ApJ, 616, 752
Martin, C. L. 2006, ApJ, 647, 222
McGaugh, S. S. 1991, ApJ, 380, 140
Michel-Dansac, L., Lambas, D. G., Alonso, M. S., & Tissera, P. 2008, MNRAS, 386, L82
Montuori, M., Di Matteo, P., Lehnert, M. D., Combes, F., & Semelin, B. 2010, arXiv:1003.1374
Moustakas, J. 2006, PhD thesis, The Univ. of Arizona
Narayanan, D., et al. 2008, ApJS, 176, 331
Paturel, G., Petit, C., Prugniel, P., Theureau, G., Rousseau, J., Brouty, M., Dubois, P., & Cambrésy, L. 2003, A&A, 412, 45
Peeples, M. S., Pogge, R. W., & Stanek, K. Z. 2009, ApJ, 695, 259
Pettini, M., & Pagel, B. E. J. 2004, MNRAS, 348, L59
Rampazzo, R., Plana, H., Amram, P., Bagarotto, S., Boulesteix, J., & Rosado, M. 2005, MNRAS, 356, 1177
Rupke, D. S., Veilleux, S., & Sanders, D. B. 2005, ApJS, 160, 87
Rupke, D. S. N., Kewley, L. J., & Barnes, J. E. 2010a, ApJ, 710, L156
Rupke, D. S. N., Kewley, L. J., & Chien, L.-H. 2010b, ApJ, submitted
Rupke, D. S. N., Veilleux, S., & Baker, A. J. 2008, ApJ, 674, 172
Sakamoto, K., Okumura, S. K., Ishizuki, S., & Scoville, N. Z. 1999, ApJS, 124, 403
Shaver, P. A., McGee, R. X., Newton, L. M., Danks, A. C., & Pottasch, S. R. 1983, MNRAS, 204, 53
Sheth, K., Vogel, S. N., Regan, M. W., Thornley, M. D., & Teuben, P. J. 2005, ApJ, 632, 217
Sol Alonso, M. S., Michel-Dansac, L., & Lambas, D. G. 2010, A&A, 514, 57
Spergel, D. N., et al. 2003, ApJS, 148, 175
Springel, V., Di Matteo, T., & Hernquist, L. 2005, ApJ, 620, L79
Trancho, G., Bastian, N., Miller, B. W., & Schweizer, F. 2007, ApJ, 664, 284
Woods, D. F., Geller, M. J., & Barton, E. J. 2006, AJ, 132, 197

Cume 355 is based on the paper *"Metallicity Gradients and Gas Flows in Galaxy Pairs"*, by Lisa Kewley etal., 2010, ApJ 721, L48. Exam prepared by R. Walterbos.

Please answer the following questions, carefully explaining each answer.

Total number of points: 65
Expected passing grade: 45

1a. (5 pts) In the introduction they mention that large, interaction-induced gas flows would dilute the central metallicity of luminous galaxies. Why is this so?

(Gas would likely mostly originate from outer parts of galaxies' disks, so be less metal rich and therefore dilute center)

1b. The authors write "We find that between the first and second pericenter (i.e. ~ 1Gyr), the metallicity gradient becomes significantly flattened and that the central metallicity becomes diluted by infalling low-metallicity gas." I think what they meant to say is "between the first and second pericenter passage".

(i) (5 pts) What do they mean with "peri-center passage"?

(Time between two successive closest passages of the galaxies in the encounter)

(ii) (10 pts) Show that for the galaxies in their sample, one might indeed expect of order 1Gyr to pass between peri-center passages.

(Here I simply want them to estimate an orbital time for two objects at about 25 kpc separation in a bound orbit. The separation comes from Table 1. They should estimate orbital velocities for galaxy interactions in a bound system, e.g. from considerations of velocities in the MW and Local Group).

Kepler III: $P^2 = \frac{4\pi^2 \cdot a^3}{G(m_1+m_2)}$ or e.g. orbital time for $\odot$, change mass & separation

2. In the section on observations, the authors discuss the number of lines per mm for the red and blue grating or grism, and then state the spectral resolution for the two sides.

a. (5 pts) What is a "dichroic"? Why would it be used?

(An optical element that splits the light into a red and a blue beam. This is a fairly common configuration for an optical spectrograph to maximize spectroscopy in blue and red. For example, it allows for a high dispersion to fit on modest size CCDs and can employ CCDs and optics optimized for either red or blue light. It also avoids overlapping orders for medium dispersion spectrographs).

b. (10 pts) The number of lines per mm is the parameter that controls the dispersion of the spectroscopic setup; think of this as over how wide an angle the light is dispersed as a function of wavelength. This, with the rest of the spectrograph optics and the details of the CCD detector determines how many Angstroms per pixel we get. In imaging, we would talk about the plate scale: how many arcsec per pixel. More dispersion implies fewer Angstroms per pixel. A related, but different, parameter is the resolution of the spectrograph, which determines how well we can resolve spectral lines (the equivalent quantity in imaging is the Point Spread Function, or PSF). The resolution is affected by the dispersion but also by other parameters, most notably for a given spectrographic setup, by the slit width used.

(i) Draw a sketch of a spectrum with some emission lines in it and indicate what is meant with the resolution and how we would measure it from the spectrum to determine it.

(The FWHM of an unresolved spectral line, e.g. a arc line from a HeNeAr lamp, or a narrow sky line)

(ii) Why do we generally use a slit with a spectrograph? What would a slit-less spectrum of an observation of a region of the sky with stars and galaxies in it look like?

(Each object would produce a spectrum on the detector, and the spectra from difference objects, which would all be parallel to each other, would likely overlap. The sky spectra would also overlap, producing one broad sky continuum background).

(iii) If I increase the number of lines per mm on a grating, does the spectrograph's dispersion go up or down (if we observe in the same spectroscopic order)? You might draw a sketch to help explain your answer. How would that generally affect the resolution?

The dispersion would increase, the closer the spacing of the lines, the further in angle the light is dispersed. This generally leads to an improvement in the resolution, at the expense of less coverage in wavelength on the detector.

(iv) How does the resolution of a spectrum change with the width of the slit (i.e. does it generally get better or worse when I observe with a wider slit)? Explain.

(A wider slit will produce lower resolution spectra if the source fills the slit width. The light in the slit is imaged onto the detector after being dispersed. Imagine two closely spaced sources on the sky, next to each other in a direction perpendicular to the slit length, just fitting across the slit width. Each source will produce a spectrum at a slightly different position on the detector. The two spectra are closely spaced on the detector in the direction of the dispersion, so effectively produce a single wider spectrum. If the seeing is such that a source does not fill the slit, the resolution would not be reduced by the slit width; in that case all the wider slit does is let more sky in, so the sensitivity will be reduced by adding sky noise. Ideal observing of unresolved sources would always require a slit width matched to the PSF)

c. (5 pts) Why do the observed spectra need to be corrected for extinction? What type of extinction(s) can you think of and how do they affect the spectra?

(There are two types of extinction, atmospheric extinction and extinction due to interstellar dust anywhere along the line of sight to the source (Milky Way dust, internal dust to in the galaxies). Both types of extinction cause suppression of the blue side of the spectrum compared to the red side and therefore this needs to be corrected for if one is interested in comparing line flux ratios from lines that occur across a range in wavelength.)

3. In section 3, the authors discuss the distances of the HII regions. They refer here to the distance of an HII region to the center of the galaxy it belongs to. They write "Our distances take inclination into account using the optical diameters, inclinations, and line-of-nodes position angles from Hyperleda ...." For line of nodes here, you can simply think of "the major axis of a galaxy on the sky".

a. (5 pts) Sketch the geometry, indicating inclination, and line of nodes. Let's say that an HII region has coordinates (ρ,ϑ) on the sky, where the center of the galaxy is at (0,0), ρ is the angular distance from the galaxy center to the HII region, and ϑ is the angle between the line of nodes (which runs through the galaxy center of course) and the line between HII region and galaxy center.

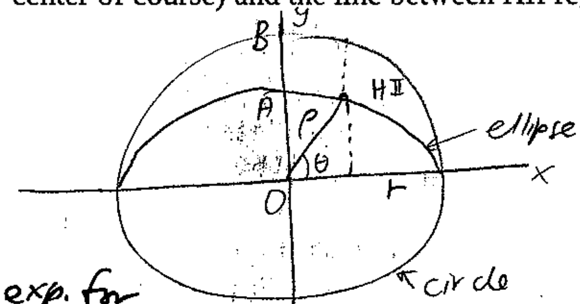

$$\frac{OA}{OB} = \cos i \left(= \frac{r\cos i}{r}\right)$$

side view:

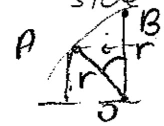

Derive exp. for

b. (5 pts) ~~Calculate the~~ radial distance r, which is the distance of the HII region to the galaxy center in the plane of the galaxy, for the HII region at (ρ,ϑ) in a galaxy with an inclination i. You should find: $r = \rho\sqrt{\left(\cos^2\theta + \frac{\sin^2\theta}{\cos^2 i}\right)}$

(For a. and b.: This is a very basic situation of an ellipse fitting inside a circle. The major axis is the galaxy's major axis. The circle is how the galaxy would appear if face-on, and has radius r. The ellipse how the galaxy appears due to its inclination to the plane of the sky. The correction from observed angular separation, rho, to radius r, for inclination simply involves increasing all "y" coordinates with a factor 1/cos(incl), where y is the direction of the ellipse's minor axis.)

c. (5 pts) For which angle theta is the uncertainty in the derived r the largest? For what range of inclination is the uncertainty highest, for inclinations between 5 to 15, or between 70 to 85. Comment.

(The correction is largest for theta approaching 90 degrees (points close to the minor axis). And it is worse as inclination approaches 90 degrees.)

4. Let's look at the results.

a. (5 pts) Why do they define the results in terms of the slope as defined in Table 1, footnote d. In particular, why do they divide the metallicity slope by (delta R/R_25)? Couldn't they have just used delta_R instead? What do they do with that parameter in the analysis?

(They want to compare gradients in different galaxies, to they normalize all radii to a dimensionless radius, defined as r over the optical radius at the 25 mag/arcsec2 level.)

b. (5 pts) Why are the inclinations relevant to the topic of this paper? Comment on this as a potential source of uncertainty on the results, considering for example what you see in the grey-scale panels in Figure 1.

(The derived abundance gradients involve knowledge of the actual radial distance in the galaxy, so they must know the inclinations of the galaxies. Given how disturbed some of these systems are, inclinations may be quite uncertain in some cases, hence so must be the radial distances for the individual HII regions in each galaxy. It is not obvious, however, how that would lead to flattening of the gradients, since an error in the adopted inclination error could go both ways. One issue that might matter is that the galaxies may not be co-planar disks anymore, in which case there is not one inclination, nor a way to derive a radial distance for an HII region.)